Research Article

Journal of Molecular Recognition

Received: 22 February 2014, Revised: 25 June 2014, Accepted: 28 June 2014, Published online in Wiley Online Library

(wileyonlinelibrary.com) DOI: 10.1002/jmr.2411

RACK1 (receptor for activated C-kinase 1) interactions with spectrin repeat elements

Line M. Myklebust*, Ole Horvli and Arnt J. Raae*

Receptor for activated C-kinase 1 (RACK1) is an intracellular scaffolding protein involved in a multitude of signalling pathways. The cytoskeleton is fundamental for intracellular cell signalling as it forms an interconnected network of regulatory proteins. Here, spectrin is a central component as it forms the actin–spectrin network that serves as docking surfaces for cellular components. The interaction between RACK1 and components of spectrin, the single spectrin repeats R16, R17 and the double spectrin repeat R1617 from the α-spectrin chain were investigated by biosensor technology and docking analysis. RACK1 associated only weakly to R16 ($K_D = 1.0 \pm 0.5 \times 10^{-6}$ M), about 20 times stronger to R1617 ($K_D = 5.3 \pm 0.7 \times 10^{-8}$ M) and 100 times stronger to R17 ($K_D = 0.9 \pm 0.3 \times 10^{-8}$ M). Docking analysis showed that while R16 alone preferentially docked with its B-helix, R17 docked through its A-helix and BC loop. The double repeat and RACK1 mainly formed two different complex conformations. R1617 docked tangentially to the N/C-terminal of RACK1 or radially along a groove on the outer surface of RACK1. These configurations could account for the slight increase in entropic and the decrease in enthalpic interactions for the R1617–RACK1 interaction, compared with the interactions of RACK1 to the two single repeats. Our results suggest a mode of interaction that allows spectrin to attach to the N/C part of RACK through the inter-helical AB and BC loops and adopt a multitude of configurations in between the two limiting configurations. Copyright © 2014 John Wiley & Sons, Ltd.
Additional supporting information may be found in the online version of this article at the publisher's web site.

Keywords: RACK1; SR (spectrin repeats); biosensor; SPR (surface plasmon resonance); binding kinetics; thermodynamic analysis and molecular docking

INTRODUCTION

The cytoskeleton is of fundamental importance for the signalling system of the cell as it forms the basic mould for coherent network of interacting molecules from the cell membrane through the cytoplasm to the nucleus. Spectrin is a key component in this system by cross-linking actin and thereby forming the actin–spectrin network (Hartwig, 1994; Viel and Branton, 1996).

Spectrin is tetrameric and consists of two α-spectrin chains and two β-spectrin chains joined together so that it forms an elongated rod-like molecule (Elgsaeter *et al*., 1986) with actin-binding domains at both ends (Begg *et al*., 2000). The major components of the spectrin chains are the so-called spectrin repeats. The α-spectrin chain consists of 21 repeats while the β-spectrin chain possesses 17 such repeats. The spectrin repeats vary in sequence similarities but have very similar 3D structures (Pascual *et al*., 1996; Grum *et al*., 1999). Basically, they are left-handed α-helical coiled coils of approximately 106 amino acid residues. The basic unit starts with the A-helix of approximately 25 amino acids followed by the AB loop that continues in the B-helix and folds back on the A-helix. The B-helix ends in the 8–12 membered BC loop and continues in the C-helix that folds back and completes the typical three-helix bundle of the spectrin repeat. The spectrin repeats are connected through a five-residue linker helix. Some spectrin repeats possess specific functions such as forming a Src homology 3 (SH3) domain, a plekstrin homology (PH) domain, and an ankyrin-binding domain (Speicher *et al*., 1992; Bennett and Gilligan, 1993; Hartwig, 1994; Begg *et al*., 2000). Additionally, spectrin repeats in general have been implicated to serve as docking surfaces for many other cellular components including both proteins (Djinovic-Carugo *et al*., 2002) and lipids (Sikorski *et al*., 2000; Diakowski *et al*., 2006).

Receptor for activated C-kinase (RACK1) is a ubiquitously conserved protein that is found in all eukaryotic cells. RACK1 has been identified as an intracellular scaffolding protein, providing a platform for protein–protein interactions, and is involved in a multitude of signalling pathways regulating cell development, growth, adhesion, motility, apoptosis, developmental processes, stress responses, neuronal activity as well as regulating transcription and translation (Battaini *et al*., 1997; McCahill *et al*., 2002; Shor *et al*., 2003; Gerbasi *et al*., 2004; Battaini and Pascale, 2005; Sklan *et al*., 2006; Arimoto *et al*., 2008; Mamidipudi and Cartwright, 2009; Subauste *et al*., 2009; He *et al*., 2010).

The 3D structure of RACK1 has been determined from plant (Ullah *et al*., 2008), yeast (Coyle *et al*., 2009), and recently, human RACK1 was determined by X-ray crystallography (Ruiz Carrillo *et al*., 2012). The structure grossly confirmed earlier homology models, based on the 3D structure of transducin (Gaudet *et al*., 1996; Sondek *et al*., 1996). RACK1 is built as a seven bladed β-propeller, each blade containing a so called WD40 sequence motif counting 40 amino acids and containing a glycine–histidine dipeptide at the N-terminal and a tryptophane-aspartic acid dipeptide at the C-terminal end (Rodriguez *et al*., 1999).

* *Correspondence to: L. M. Myklebust and A. J. Raae, Department of Molecular Biology, University of Bergen, HIB, Thormoehlens gt. 55, N-5020 Bergen, Norway. E-mail: Line.Myklebust@mbi.uib.no; arnt.raae@mbi.uib.no*

L. M. Myklebust, O. Horvli, A. J. Raae
Department of Molecular Biology, University of Bergen, HIB, Thormoehlens gt. 55, N-5020 Bergen, Norway

The cellular role of RACK1 is still not fully known, but RACK1 has been identified as a stoichiometric ribosomal protein associated to the small ribosomal subunit both in eukaryotes and yeast (Sengupta *et al*., 2004; Chandramouli *et al*., 2008; Ben-Shem *et al*., 2010; Rabl *et al*., 2011). The positioning immediately adjacent to the 3′ mRNA exit channel may link RACK1 to a key role in the regulation of protein synthesis (Guo *et al*., 2011).

RACK1 has been identified as a binding partner for numerous proteins and more than 85 entries are currently reported in the Biomolecular Object Network Databank (BOND), (http://bond.unleashedinformatics.com/Action). Especially, signalling factors have been identified as RACK1 binding partners (Steele *et al*., 2001; Battaini and Pascale, 2005; Onishi *et al*., 2007; Kundu *et al*., 2013). RACK1 binding to β-spectrin was reported by Rodrigues and co-workers (Rodriguez *et al*., 1999) and represent one of few detailed molecular analyses of the binding of RACK1 to other proteins. Another study investigated the interaction of RACK1 to the phosphodiesterase PDE4D5 (Smith *et al*., 2007). One reason for the lack of kinetic interaction analysis is that RACK1 is relatively unstable upon purification (Bjørndal *et al*., 2003) and is difficult to keep in solution in a stable, soluble form.

By pull-down analysis, we previously found that a minispectrin, consisting of the actin-binding domains and the two first spectrin repeats of the α and β chains respectively (Raae *et al*., 2003), associated weakly to RACK1. Hence, to analyse the interaction to RACK1 in more detail, we choose the structurally well-characterised single spectrin repeats R16 and R17 from the α-spectrin chain together with the double repeat R1617 as interaction partners. These molecules could be produced in ample amounts and were highly soluble and stable in contrary to larger constructs of spectrin showing decreased solubility (Lenne *et al*., 2000). Moreover, the spectrin repeat molecules contain the basic structural components of the spectrin chain such as the three A, B and C helices with connecting loops and the linker region between two neighbouring spectrin repeats (R1617) that all could be possible targets for protein–protein interactions in the spectrin chain. Using surface plasmon resonance (SPR) technology, we obtained detailed binding kinetic data and thermodynamic parameters for the interactions. We found that the single spectrin repeat R16 associated weakly to RACK1 whereas the double repeat R1617 and R17 bound about 20 and 100 times stronger to RACK1, respectively. Thermodynamic analysis of the R1617 interaction with RACK1 suggested a dominating enthalpic component of the interaction through R17 and a possible entropic component through R16. Docking analysis showed that R17 could interact through more amino acid residues compared with R16 and R1617, and this is in concordance with the SPR affinities detected for R17, where R17 interacts strongest with RACK1 among the spectrin repeat elements tested. Taken together, our data suggests a model for RACK1 association in the cytoskeleton/membrane system.

MATERIALS AND METHODS

Proteins

Human RACK1 fused to maltose-binding protein (MBP) was hetereologously expressed in *Escherichia coli* and prepared as described earlier (Bjørndal *et al*., 2003; Bjørndal *et al*., 2007). The genes for R1617 and R17 were PCR cloned from chicken organ full-length complementary DNA (brain) from Seegene Inc. and further processed into a pET12 vector (a generous gift from G. Stier) and expressed in *E. coli* BL-21 cells.

SPR measurements

The SPR measurements were carried out on a Biacore T-100/T-200 instrument (GE-Healthcare) using CM5 chips. The CM5 sensor chips were preconditioned (3× 10 s injections of running buffer (1× HBS-EP: 10 mM Hepes, pH 7.4, 0.15 M NaCl, 3.4 mM EDTA and 0.05% surfactant P20), 2× 10 s injections of 100 mM HCL, 2× 10 s injections of 50 mM NaOH followed by 2× 10 s injections of 0.5% sodium monododecyl sulfate with a flow of 100 μl/min). For amino coupling of the ligands, a typically 1:1 mixture of *N*-ethyl-*N*′-(3-dimethylaminopropyl) carbodiimide hydrochloride (from Pierce) and *N*-hydroxysuccinimide (from Pierce) was injected for 420 s with a flow of 5 μl/min to create reactive succinimide esters before injection and covalent immobilization of the ligand. All unreacted esters after immobilization of the ligand were blocked with a 420 s injection of ethanolamine-HCL (flow; 5 μl/min). RACK1 was used as ligand whereas the spectrin repeats R16, R17 and R1617 were used as analytes. Typically freshly purified RACK1, 0.1 mg/ml, was either amino coupled to the CM5 chip at a flow rate of 10 μl/min for 1 min. at room temperature or captured on amino-coupled anti-RACK1 (B3, Santa Cruz Biotechnology) on the CM5 chip. To note, all figures in the manuscripts are made on antibody captured RACK1 protein as ligand on the sensor chip. The ligands were routinely coupled to the sensor chip surfaces at densities between 100 and 200 RU on FC-2 and 800 and 1000 RU on FC-4 respectively. FC-1 and FC-3 functioned as negative controls and were treated as FC-2 and FC-4 except that no ligand was coupled to the surfaces.

The analyte concentrations were varied between 20 and 6000 nM and flowed over the ligand surfaces at a flow rate of 60 and 100 μl/min to avoid mass transport. The chip surfaces were regenerated by flowing buffer at 30 μl/min for 10 to 30 min between the different cycles of analyte applications. Control SPR analysis at 25°C was performed with RACK1, RACK1 fused to MBP and MBP-fused spectrin repeats. The interaction analysis between RACK1 and the spectrin repeats were extensively repeated several times at the same conditions (antibody capturing of RACK1 or directly immobilised RACK1) with different protein batches of both RACK1 and the spectrin repeats. Also, the binding analyses were carried out with different SPR procedures such as single- and multi-cycle kinetics. The experiments were always carried out by using RACK1 as the immobilised ligand. This was in order to achieve optimal stabilisation of the experimental system as binding in general is supposed to stabilise the binder (Creighton, 1997).

The SPR sensorgrams were fitted to different interaction models (Figure S2). As shown in Figure S2, the simple 1:1 model fitted practically equally well as the other more complex interaction models. Therefore, the binding strength of the spectrin repeats–RACK1 interactions was assessed by global fitting of the sensorgrams to a 1:1 Langmuir interaction model. In global fitting, the association and dissociation phase are evaluated simultaneously for optimal generation of the kinetic values.

The thermodynamic parameters were obtained from binding experiments carried out at 10, 15, 25 and 35°C. The data were analysed with the Biacore evaluation software 2.0.1 and a global fitting of the sensorgrams to a 1:1 Langmuir interaction model. Thermodynamic parameters were calculated according to equations and methods described in the GE Healthcare

Journal of Molecular Recognition

Application Note 80 for Biacore systems: Transition state thermodynamic analysis using Biacore T100 (https://www.biacore.com/lifesciences/technology/application_notes) (GE Heathcare), Shuman *et al.* (Shuman *et al.*, 2004) and Navratilova *et al.* (Navratilova *et al.*, 2007). The thermodynamic parameters were generated from the van't Hoff and Eyring plot options in the Biacore evaluation software 2.0.1.

Homology modelling

RACK1 was homology modelled using the RACK1 structure of *Arabidopsis thaliana* (pdb: 3 dm0) as template using the Swiss PDB Viewer software (http://spdbv.vital-it.ch/).

The RACK1 model was compared with the human RACK1 crystal structure (4aow) by using the Molsoft software ((Molsoft L.L.C.), http://www.molsoft.com/), which also was used to produce the protein structures and to analyse the docking complexes.

Molecular docking

Molecular interaction docking analysis was basically carried out by two complementing softwares: the Gramm-x docking software ((Tovchigrechko and Vakser, 2006), http://vakser.bioinformatics.ku.edu/resources/gramm/grammx) to perform global searches for the best rigid body conformations and the PatchDock software ((Schneidman-Duhovny *et al.*, 2005), http://bioinfo3d.cs.tau.ac.il/PatchDock/) that samples for shape complementarity. Supportive docking analysis were carried out with the ZDOCK server ((Pierce *et al.*, 2014), http://zdock.umassmed.edu/) and with the Molsoft software ((Molsoft L.L.C.), http://www.molsoft.com/). The 3D structures of R16 and R17 were based upon the crystal structure of R1617 (Pdb file:1CUN) and used for the molecular docking analyses.

RESULTS

RACK1 and the spectrin repeats

The structures of the spectrin repeats and RACK1 are shown in Figure 1. The spectrin repeats and their structural elements: the three A, B and C helices are connected by the A-B and the B-C loops that folds back upon each other to form a helix bundle (Figure 1A–C). All spectrin repeats contain the so-called five-residue linker helix (Grum *et al.*, 1999) that forms the C-terminal in R16 and the N-terminal in R17 and hence is the linker between the two spectrin repeats in R1617. Figure 1D shows the top view of RACK1 with the seven Trp-Asp (WD) propeller blades and the co-localization of the N- and C-terminals between blades 1 and 7.

The insert in Figure 1D (refer to enlarged figure in supplementary Figure S1) shows a comparison between the RACK1 homology model (red trace) and the human crystal structure (blue trace). The weighted root mean square deviation (RMSD) for the two structures was 0.29 Å and thus reflects that only minor differences exist between the two structures. As most of the docking data was obtained using the homology model of RACK1, we show that our homology model is nearly identical to the recently published crystallographic 3D structure (Ruiz Carrillo *et al.*, 2012). For

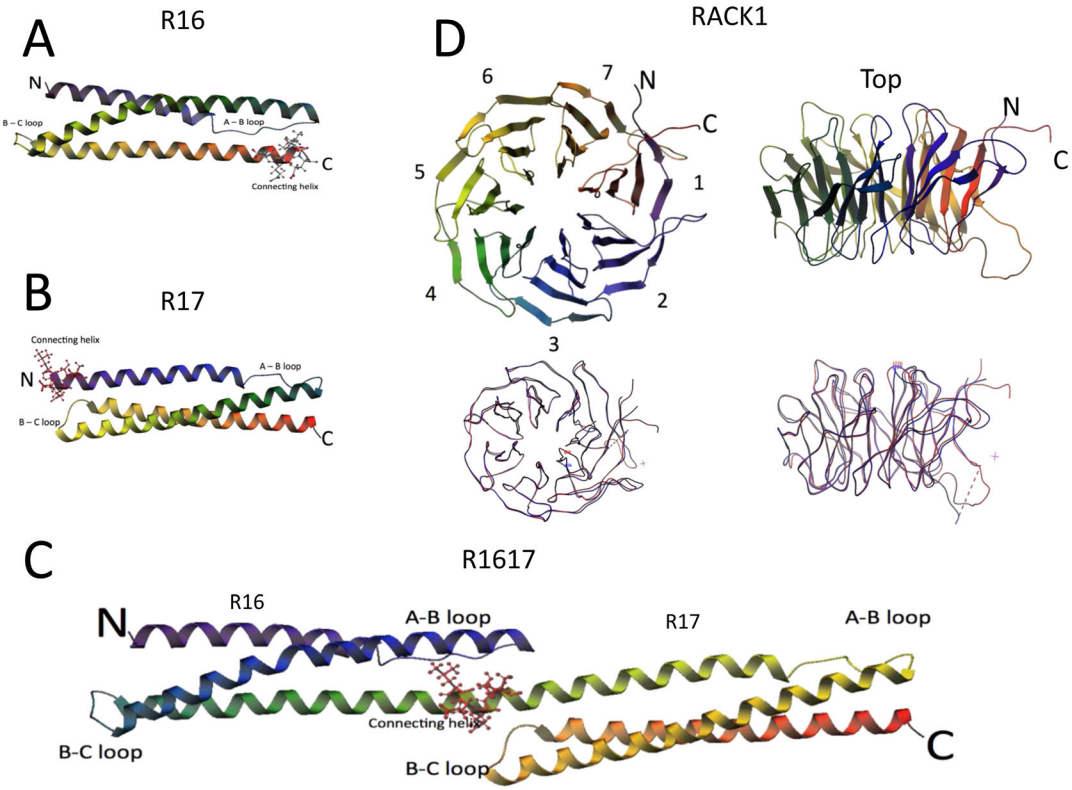

Figure 1. 3D structures of the interacting molecules RACK1 and the spectrin repeats. Schematic representations of the interacting molecules; R16 (A) and R17 (B) with the A, B and C helices and the AB and BC loops indicated. In R1617 (C), R16 is connected through a five residue 'connecting helix' that divides the long continuous helix into the C-helix of R16 and the A-helix of R17. For RACK1 (D), the WD-propeller blades are numbered from 1 to 7. The seventh propeller blade is constituted by that the N-terminus forms the outer strand of the blade while the inner part is formed by the C-terminus. For all structures, the N-terminus is coloured blue and the C-terminus red. An insert to panel D shows a comparison between our homology model (red trace) and the hRACK1 crystal structure (4aow, blue trace).

comparative purposes, 35Q is labelled in the model and in the X-ray structure as this residue in few areas show minor divergences between the two structures.

RACK1 interacts strongest with the spectrin repeat R17

The sensorgrams of RACK1 binding to the single spectrin repeats R16 and R17 are shown in Figure 2A and B, respectively. The SPR sensorgrams were fitted to different interaction models (shown in Figure S2). The interaction strength (K_D) is the ratio between the dissociation rate constant k_d and the association rate constant k_a. We found that R16 bound to RACK1 with a K_D of $1.0 \pm 0.5 \times 10^{-6}$ M and R17 bound about 100 times stronger with a K_D of $0.9 \pm 0.3 \times 10^{-8}$ M.

The sensorgram of the binding of R1617 to RACK1 is shown in Figure 2C. The interaction strength was determined to a K_D of $5.3 \pm 0.7 \times 10^{-8}$ M, which is about 20 times stronger than R16 but 5 times weaker compared with R17.

Inspection of the sensorgrams in Figure 2 indicates differences in the interaction kinetics between the spectrin repeats. The association of R17 to RACK1 produces nearly linear association phases, especially at low analyte concentrations, whereas the association of R16 is fast and proceeds steeply in the beginning and tends to flatten out at the end of the association phase. The association phase of the R1617 to RACK1 interaction proceeds in a manner in between the association of the two single repeats to RACK1.

Thermodynamics of the spectrin repeat–RACK1 interactions

Thermodynamic analyses of the interactions of R16, R17 and R1617 to RACK1 were carried out at four different temperatures; 10, 15, 25, and 35°C (Figure 3). The sensorgrams show that all reactions were affected by the different assay temperatures. Especially, changes in the association phase of the sensorgrams were apparent. The binding kinetics of R16 and R17 seemed to be more affected by the temperature changes compared with R1617. For R16, the association curve approached saturation (flattens out more) at the lowest temperature, 10°C, compared with the steeper association phases at the highest temperature, 35°C. The sensorgrams for R17 differ substantially as the association curves proceeds more linearly with a slight tendency to flatten out at the end of the association phase at the lowest temperature (10°C). This was followed by steeper association curves at increasing temperatures that could reflect increasing interaction strength. The sensorgrams for the R1617 to RACK1 association showed little or no such changes in association phase curvature. This indicates that the three interactions were governed by different enthalpic and entropic contributions. Thus, the apparent increase in interacting strength for R16 and R17 could reflect hydrophobic effects governed by the R16–RACK1 and R17–RACK1 interactions. An alternative explanation could be that thermo-instability of R17 (Tm 31°C) could cause avidity and/or rebinding phenomena at increasing temperatures.

R16, R17 and R1617 interact with RACK1 with different enthalpic and entropic contributions

From the thermodynamic analysis of the interactions between RACK1 and the spectrin repeats R16, R17 and R1617 (Figure 3), the standard thermodynamic parameters (ΔH°, ΔS° and ΔG°) and transition state parameters for the association phase (ΔH°$^{\#}$,

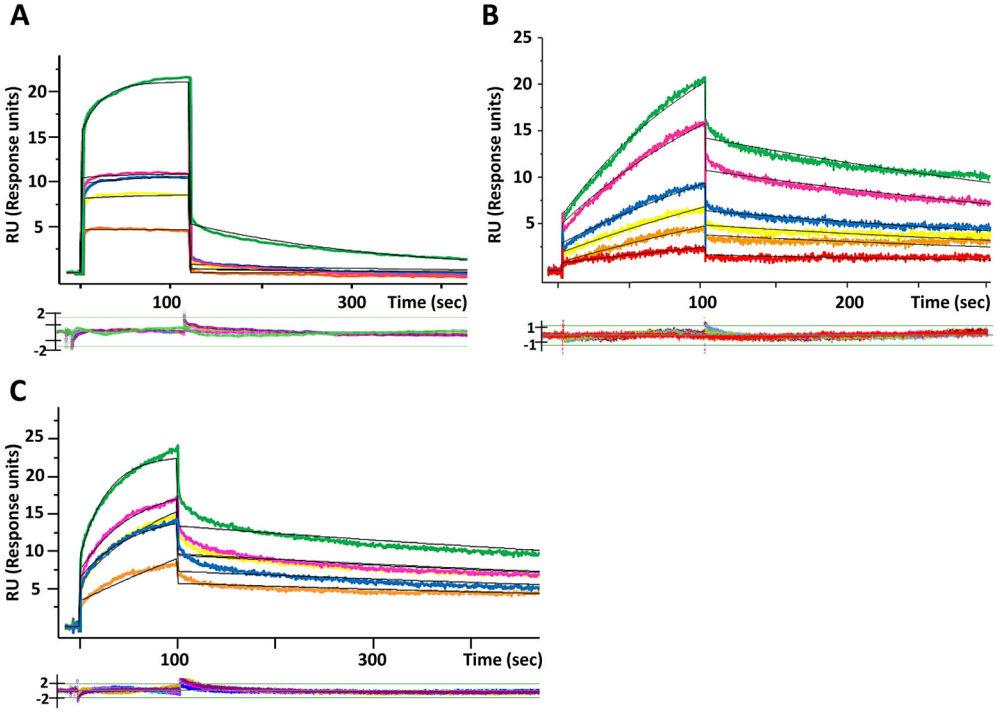

Figure 2. Sensorgrams of spectrin repeat interaction with RACK1. SPR analyses were performed at 25°C to measure the interaction strength of different spectrin repeats with RACK1. The sensorgrams for the spectrin repeat R16 (A), R17 (B) and R1617 (C) to RACK1 is shown. Different concentrations of analyte, 0 to 6000 nM, were passed over a sensor chip surface of 100 RU antibody captured RACK1 as ligand. Concentrations of R16: 5000 nM (green), 2000 nM (pink), two times injection of 1000 nM (blue and yellow) and 500 nM (orange). Concentrations of R17: 6000 nM (green), 4000 nM (pink), 2000 nM (blue), 1000 nM (yellow), 600 nM (orange) and 200 nM (red). Concentrations of R1617: 2000 nM (green), 1000 nM (pink), two times injection of 500 nM (blue and yellow) and 100 nM (orange). The sensorgrams were fitted to the 1:1 Langmuir binding model (indicated with a black sensorgram line).

Journal of Molecular Recognition

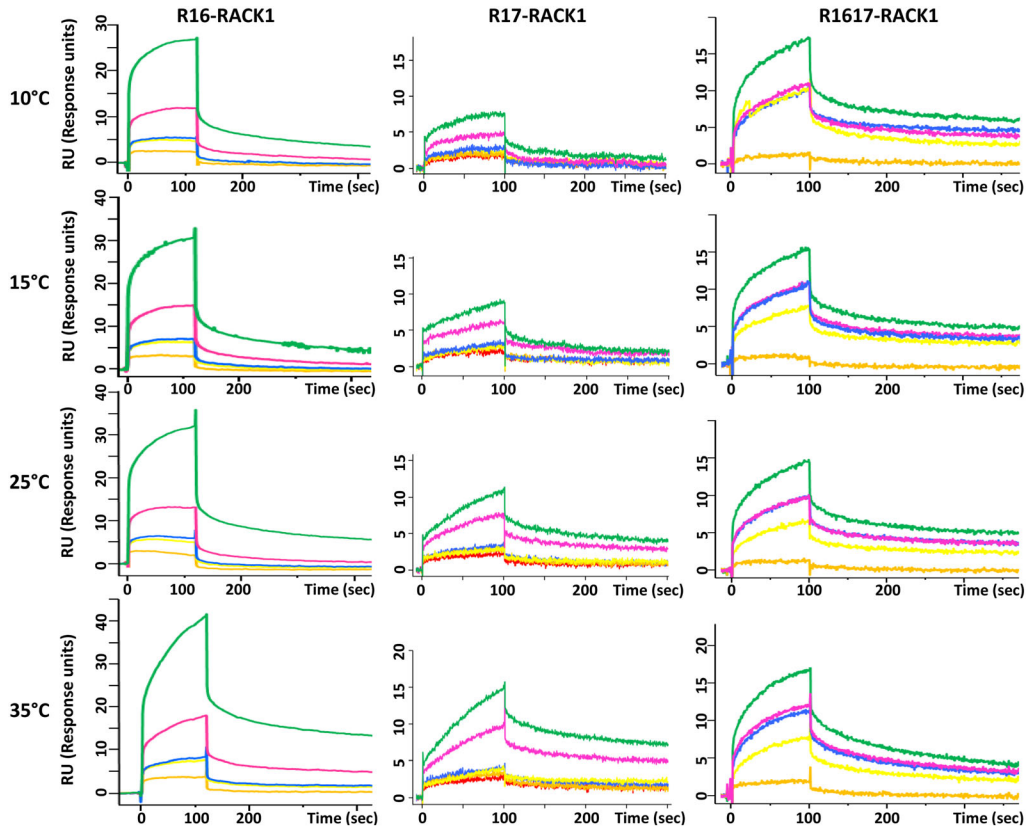

Figure 3. SPR analyses of spectrin repeat interaction with RACK1 at different temperatures. SPR analyses were performed to measure the interaction strength of different spectrin repeats with RACK1 at 10, 15, 25 and 35°C. Typical sensorgrams for the interaction of spectrin repeat element R16, R17 and R1617 with RACK1 is shown. Different concentrations of analyte, 0 to 6000 nM, were passed over a sensor chip surface of 100 RU antibody captured RACK1 as ligand. For R16: 5000 nM (green), 2000 nM (pink), two times injection of 1000 nM (blue and yellow) and 500 nM (orange). For R17: 6000 nM (green), 4000 nM (pink), 2000 nM (blue), 1000 nM (yellow), 600 nM (orange) and 200 nM (red). For R1617: 2000 nM (green), two times injection of 1000 nM (pink and blue), 500 nM (yellow) and 100 nM (orange). The thermodynamic parameters were obtained by global fitting of the sensorgrams according to the 1:1 Langmuir binding model.

$\Delta S^{\circ\#}$ and $\Delta G^{\circ\#}$) were extracted and listed in Table 1. There were only small differences in the free energy changes for the interactions (Table 1). The ΔG° for the R16–RACK1 interaction was −27 kJ/mol compared with 34 and 39 kJ/mol for the R17 and R1617 interactions with RACK1, respectively. However, the changes in the enthalpies and entropies for the interactions showed substantial differences. The ΔH° and $T\Delta S^\circ$ values for the R17–RACK1 and R1617–RACK1 interactions were comparable and were −33 and 4 and −21 and 18 kJ/mol for the R17–RACK1 and R1617–RACK1 interactions, respectively. The RACK–R16 interaction differed substantially and showed a ΔH° of 74 kJ/mol and a $T\Delta S^\circ$ value of 100 kJ/mol.

The differences in the transition state thermodynamic parameters for the reactions are visualised in Figure 4. At the *x*-axis of the figure is the reaction coordinate—that is a schematic view of the state of interaction parameters during the course of the interaction. On the *y*-axis are the values of the thermodynamic parameters for ΔG°, ΔH° and $-T\Delta S^\circ$ plotted. First, the changes in the thermodynamic parameters are set to zero before the interaction of RACK1 and spectrin starts (initial state indicated as RACK1 + spectrins in Figure 4). Second, the changes in the thermodynamic parameters for the interacting complex, (RACK1–spectrin)*, are data collected from the transition state values in Table 1), and third, the changes in the thermodynamic

Table 1. Thermodynamic parameters for the interaction between RACK1 and the spectrin repeats R16, R17 and R1617

	Thermodynamic parameter	R16	R17	R1617
Standard thermodynamic parameters	ΔH° (kJmol^{-1})	74 ± 10	−33 ± 10	−21 ± 10
	ΔS° (J(K mol^{-1}))	340	4	38
	ΔG° (kJ mol^{-1})	−27 ± 1	−34 ± 1	−39
	$T\Delta S^\circ$ (kJ mol)	100 ± 10	4 ± 1	18 ± 10
Transition state association parameters	$\Delta H^{\circ\#}$ (kJmol^{-1})	8 ± 6	−60 ± 10	−3 ± 1
	$\Delta S^{\circ\#}$ (J(K mol^{-1}))	−183 ± 35	−383 ± 35	−180 ± 14
	$\Delta G^{\circ\#}$ (kJ mol^{-1})	63 ± 1	55 ± 3	50
	$T\Delta S^{\circ\#}$ (kJ mol)	−55 ± 10	−110 ± 10	−53 ± 5

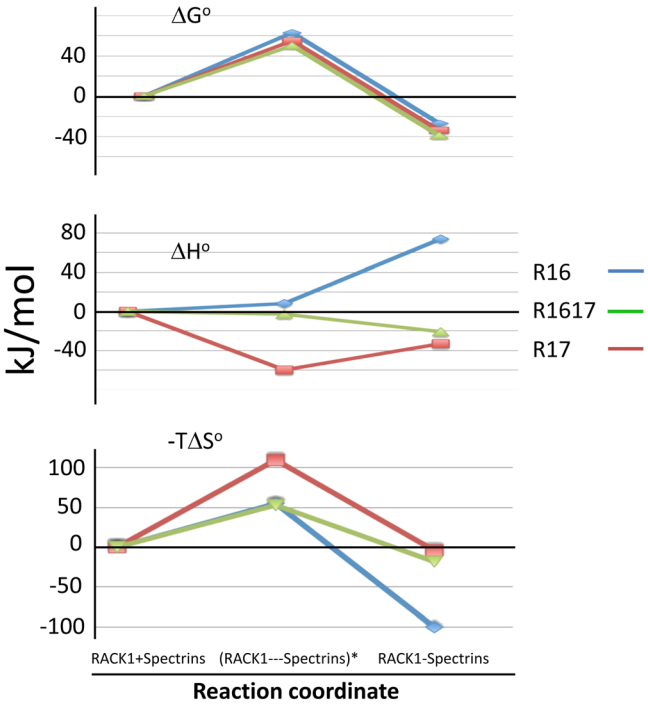

Figure 4. Thermodynamic analysis of RACK1 interaction with R16, R17 and R1617. Shown in the figure is the reaction coordinate plotted against the values for ΔG°, ΔH° and TΔS° (data from Table I). The initial state represents the spectrin repeats and RACK1 before interaction (indicated with RACK1 + spectrins). The transition state represents the complex formation (RACK1–spectrin)*, and the final state represents the formed RACK1–spectrin repeat complexes (RACK1–spectrins). Blue trace; R16, green; R17 and red; R1617.

parameters in the final state, the RACK1–spectrin repeat complexes, (RACK1–spectrins), are data collected from the standard thermodynamic parameters in Table 1. As can be seen from the figure, the transition state free energy changes, $\Delta G^{\circ\#}$, for the three reactions were similar. In contrast, substantial differences were seen for both the transition state enthalpies and entropies, particularly for the R16–RACK1 interaction compared with the R17–RACK1 and the R1617–RACK1 interactions.

Docking of the spectrin repeats to RACK1

Typical examples of the docking complexes are as shown in Figure 5. The docking analysis was carried out by employing complementing online docking services, one that sampled complexes based on shape complementarity (Patch Dock) and another that used charge complementarity as sampling criteria (Gramm-X). The different softwares produced grossly the same interaction structures although the relative distribution of the most significant structures varied according to the software. Patch Dock tended to yield structures where the spectrin repeats docked tangentially to RACK1 whereas Gramm-X produced complexes were the spectrin repeats bound to the outer surface of RACK1.

Interestingly, the inner or 'bottom surface' of RACK1 that is attached to the ribosome (Sengupta *et al*., 2004) was practically not observed as a docking target for the spectrin repeats.

R16 docked preferentially to the N/C-termini of RACK1 with the B-helix either tangentially or radially on the outer surface

Representative interaction complexes between R16 and RACK1 from the docking analysis are shown in Figure 5A. Mainly two types of structures appeared were R16 interacted through the B- and C-helices either radially on the outer surface of RACK1 or tangentially to the N/C- termini of RACK1 (Figure 5A.I and II). The B-helix of R16 contains the typical kink around a histidine (H58) in a sequence stretch were the amino acids that lie less than 5 Å apart from RACK1 were of an overall hydrophobic character; A53, A56, A57 and P60 (refer to Figure S3 for possible interacting amino acids). This region attached tangentially the B-helix near the N/C-termini and the propeller blades 6 and 7 of RACK1. On the surface of RACK1, the helices B and C tended to align along a putative surface groove, which roughly divides the RACK1 surface so that blade 1, 2 and 3 are on one side and 4, 5, 6 and 7 are on the other side. However, structures where R16 aligned perpendicular to this groove, as shown in Figure 5A.I, were also seen. Thus, the docking analysis showed that R16 docked to RACK1 with a relatively large structural variety.

R17 interacts with RACK1 through its BC loop and N/C-terminus tangentially to surface residues on all WD blades in RACK1

R17 docked to the N/C-part of RACK1 by its negatively charged N-terminus (LEESLEY) and histidine-containing BC loop (NNHH). Figure 5B shows the two most occurring complex structures. Figure 5B.I and Figure 3S show that R17 bound to the outer surface of RACK1 touching the surface loops of blade 7 and 1 through the BC loop/N-terminus. In the other complexes, as shown in Figure 5B.II, R17 bound tangentially to the N/C-part of RACK1 through its BC loop/N-terminus. In the radial conformation, R17 bound to RACK to surface residues from all WD blades of RACK1 as seen from Figure S3. According to Figure S3, R17 seems to be closer to the RACK1 surface compared with R16 as R17 possesses a higher number of possible binding partners (amino acids less than 5 Å apart) compared with R16.

R17 is the only spectrin repeat with three positive charges in the BC loop (positions 81–85) as described in Brenner *et al*. (Brenner *et al*., 2012). Possible binding partners in RACK1 are the C-terminal residues IGTR (314–317) that are less than 5 Å apart from the residues in the BC loop.

R1617 interacts with the N/C-termini of RACK1 through the AB loop of R16 and the BC loop of R17 either tangentially or radially on the outer surface of RACK1

Typical docking complexes for the interaction between R1617 and RACK1 are shown in Figure 5C. The docking software produced similar complexes where R1617 bound to RACK1 through the BC loop of R17 and the AB loop of R16 to the N/C-part of RACK1 (blade 1 and 7). The positioning of R1617 relative to RACK1 varied from radially to tangentially as shown in Figure 5C.I and II.

In the tangential complex, both the AB loop of R16 and BC loop of R17 was in close contact with surface loops of blade 1 and 7 of RACK1 (Figure 5C.II and Figure S3). In the radial configuration (Figure 5C.I), the BC loop of R17 (NNHH) contacts the N/C-terminal and residues from WD blade 1 and 7 of RACK1 whereas the AB loop (VSSEDYGRD) and the C-terminal end of helix A in R16 were in contact with inner surface loops from all WD blades of RACK1 (Figure S3). In addition to this, the linker region between R16 and R17 (EESLE) may participate in the interaction between R1617 and RACK1. As seen from Figure S3, the number of possible interacting residues in the R1617–RACK1 complex (shaded residues) are fewer compared with the R17–RACK1 complex.

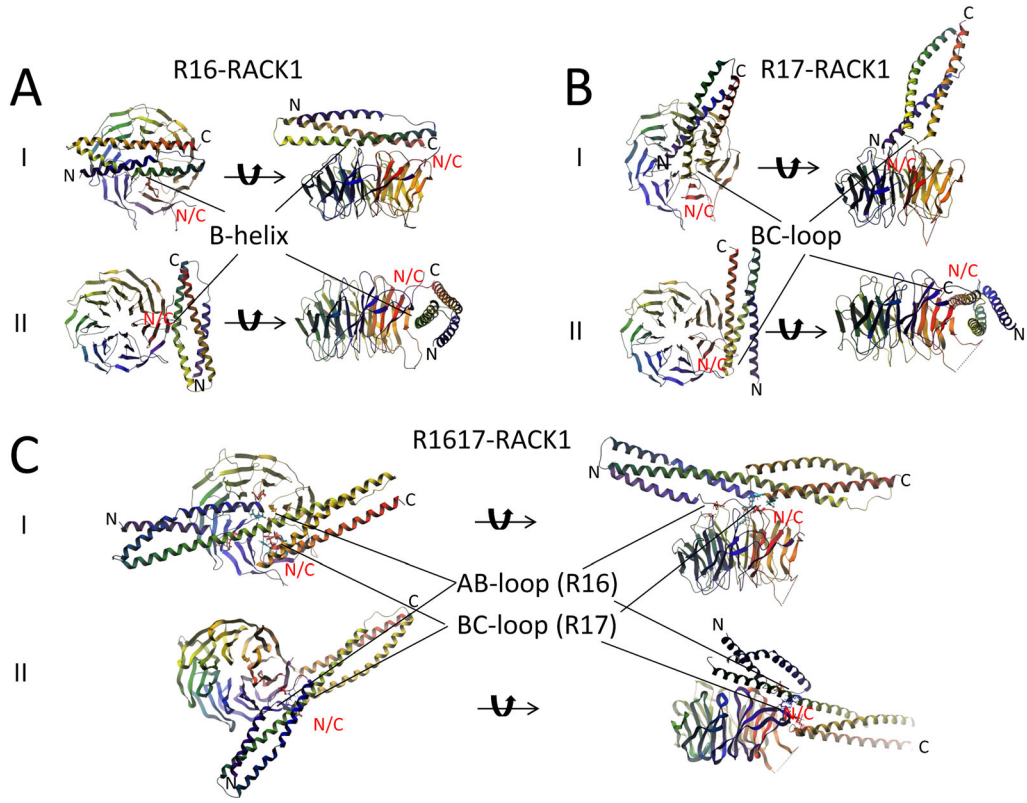

Figure 5. Representative docking complexes of RACK1 and spectrin repeats. A panel of representative spectrin repeat–RACK1 docking complexes: (A) R16–RACK1, (B) R17–RACK1 and (C) R1617–RACK1. The structures are shown as radial (I) and tangential (II). The protein structures were coloured according to structure polarity, the N-terminus coloured dark blue and the C-terminus coloured red (N to C colouring method). N- and C-terminus are indicated with black letters for the spectrin repeats and in red letters for RACK1.

DISCUSSION

So far, only few *in vitro* studies of RACK1 have been reported. A reason for this is that RACK1 has proved to be unstable and difficult to keep in solution for prolonged time (Bjørndal *et al*., 2003). In our kinetic analysis, we found that the most optimal assay system involved capture of RACK1 with an anti-RACK1 antibody. This stabilised RACK1 sufficiently so that reliable kinetic data could be obtained. For simplicity, we choose to extract the binding parameters after fitting the binding data to the simple 1:1 Langmuir interaction model. The data fitted reasonably well as shown in Figure S2. However, our data fitted slightly better to the more complex interaction models, such as heterogeneous ligand or analyte and the two-state interaction models (data not shown). The two state model is not supposed to be qualified and examined by SPR (the measurement goes on for minutes whereas conformational changes in proteins normally happens in nanoseconds/milliseconds to seconds), except for specific protein systems. Thus, the analysis should be combined with supplementary methods such as NMR (Rich and Myszka, 2010). The lack of perfect curve fitting could reflect that the scaffolding protein RACK1 possesses a more complex interaction regime or that the unstable RACK1 protein harbours surface heterogeneity or other secondary binding sites (Svitel *et al*., 2007; Rich and Myszka, 2010). However, our data fitted reasonably well to the 1:1 model; therefore, we believe that our binding data reflects realistic measures of the *in vitro* interaction strengths between RACK1 and the spectrin repeats analysed in this work.

Our findings demonstrated that RACK1 interacted weakest with R16 ($K_D \approx 1 \times 10^{-6}$ M), about 20 times stronger to the double repeat, R1617 ($K_D \approx 5.3 \times 10^{-8}$ M) and about 100 times stronger to R17 ($K_D \approx 0.9 \times 10^{-8}$ M) as compared with R16.

For comparison, other studies of RACK1 interactions by SPR includes the interaction between RACK1 and Kindilin-3 (Feng *et al*., 2012) and murine angiotensin II receptor-associated protein (Agtrap) (Wang *et al*., 2002). The interaction to Kindilin-3 was measured to have a K_D of 1.8 μM whereas for the interaction of RACK1 to murine Agtrap, only the association rate constant, 5.02×10^3 M^{-1} s^{-1}, and dissociation rate constant, 7.98×10^{-5} s^{-1}, were reported.

Compared with other interactions involving spectrin repeats, the interaction strength reported in this paper is within a similar range. The K_D of the binding of the ZU5 domain of ankyrin to the R1415 double spectrin repeat from β-spectrin was reported to vary between 10 nM (measured by electrochemiluminescence immunoassay), 40 nM (by fluorescence resonance energy transfer) (Kolondra *et al*., 2010) and 194 nM measured with isothermal titration calometry (ITC) (La-Borde *et al*., 2010). In a similar protein–protein interaction analysis, it was found that minispectrin, consisting of the CH and EF domains together with four spectrin repeats, bound to actin with a K_D of about 2.5 μM (Raae *et al*., 2003). Furthermore, it has been shown that cyclophilin A interacts with the HIV-1 virus capsid protein Vpr with a K_D of about 320 nM (Solbak *et al*., 2011).

The thermodynamic parameters (state functions) for the R17 and R1617 to RACK1 interactions were similar but differed from those of R16. As the R17 and R1617 interactions to RACK1 had

negative enthalpies, ΔH°, and small TΔS° values, R16 showed large positive values for both ΔH° and TΔS°, suggesting that the R16 interaction was dominated by entropic contributions in contrast to the R17 and R1617 interactions that were dominated by enthalpic interactions (Table 1 and Figure 4).

Also, the transition state thermodynamic parameters showed that the R16 to RACK1 interaction deviated from the others by having a small positive enthalpic increase whereas the association phase for both the R17 and R1617 interaction were characterised by large negative transition state enthalpies. This is consistent with entropic interactions dominating in the R16 to RACK1 interaction, whereas enthalpic interactions dominate in the R17 to RACK interaction. However, the RACK1–R1617 interaction had a larger entropic contribution compared with R17, which could imply a contribution from R16. Moreover, because the R17 to RACK1 interaction was about 100 times stronger compared with the R16 to RACK1 interaction, we find it highly probable that R17 plays a dominating role in the interaction of the double repeat to RACK1. The fivefold decrease in binding strength of the double repeat compared with R17 could imply that R1617 contains pure steric hindrances, imposed by R16, which reduces the binding strength of R17 to RACK1 in the R1617–RACK1 complex. Alternatively, R17 forces R16 to a less productive conformation in the R1617 interaction to RACK1. In the R16 to RACK1 interaction, R16 associated predominantly through the kinked B-helix whereas in R1617, it was frequently the opposite side, the AB loop of R16 that was in contact with RACK1 and may engage repulsive forces between RACK1 and R16.

Other workers have used a similar approach to analyse the binding of different enzyme inhibitors. Shuman *et al.* (Shuman *et al.*, 2004) used SPR methodology to characterise the interaction between HIV protease and seven inhibitors by kinetic and thermodynamic analysis. The binding constants varied from about 0.1 to 6.9 nM whereas the equilibrium ΔG for the reactions were in the range of −48 to 57 (kJmol). The equilibrium ΔH varied from about 9 to 29 (kJ mol), and the equilibrium ΔS varied between 0.220 to 0.272 kJ mol T. Also, the thermodynamic parameters for the association and dissociation phases were obtained and enabled discussion of interactions in terms of enthalpic and entropic changes such as the forming of H bonds and van der Waals interactions (negative ΔH), entropy, ΔS, changes in randomness, conformational, rotational and translational degrees of freedom as well as solvent effects. Navratilova et al. (Navratilova *et al.*, 2007) compared thermodynamic analysis using SPR technology compared with ITC. The interaction studied was between carbonic anhydrase II and four sulfonamide inhibitors. The data obtained by the two technologies correlated well and measured K_D values that ranged from about 3×10^{-5} to about 5×10^{-7} M and ΔH values from −3 to about −12 (kcal/mol).

As shown in the structure (Figure 5C.I), R1617 is attached to the N/C-termini of RACK1 by the BC loop of R17 and thereby forms a strong electrostatic interaction at the same time as the C-terminal part of R16 with the AB loop aligns along the surface groove involving residues from practically all WD blades of RACK1 (refer to Figure S3). This part of R16 was not seen bound to RACK1 in the docking analysis of RACK1 to pure R16 were the kinked B-helix bound to RACK1. This could force R17 in the R1617–RACK1 complex into an unfavourable position in the interaction to RACK1 compared with free R17 and thus presents an explanation for the reduction in interaction strength between R1617 and RACK1 compared with R17. As seen from Figure S3, the number of possible interacting amino acids is highest in the R17–RACK1 complex compared with both the R16–RACK1 and the R1617–RACK1 complex.

However, our kinetic and thermodynamic data cannot distinguish between the two complexes shown in Figure 5C. A fivefold difference in interaction strength could easily be caused by a few strong electrostatic interactions. Interestingly, the 'tangential' complex structure (Figure 5C.II) shows resemblance to structures revealed in other studies involving RACK1 and spectrin, for example, the interaction between RACK1 and PKC. Cryoelectron micrographic analysis shows that PKC aligns tangentially to WD blades 3 and 4 of RACK1 (Sharma *et al.*, 2013). Also, the so-called RACK interacting domain (RAID) is thought to interact tangentially to RACK1 involving WD blade 1, similar to the γ-transducin to β-transducin interaction (Bolger *et al.*, 2002).

The ZU5 domain of ankyrin is structurally similar to RACK1, being a β-propeller. Moreover, sequence and structural alignment of ZU5 and RACK1 revealed that the ZU5 to ankyrin-binding residues correspond to residues 2–36 on strand 4 in blade 1 of RACK1 (data not shown). Similar to RACK1, ZU5 associates to the linker region between R14 and R15 of β-spectrin involving the BC loop of R15 and the AB loop of R14 (Kolondra *et al.*, 2010). Interestingly, crystallographic analysis demonstrates that ZU5 aligns tangentially to the R1415 spectrin unit.

CONCLUSION

Our data suggests that the linker region of R1617 of the α-spectrin chain can serve as a specific binding site for RACK1 similarly to the binding of R1415 to the ZU5 domain of ankyrin and thereby provide a specific docking site for the scaffold protein RACK1 to the cytoskeleton. An alternative explanation could be that the linker regions in the spectrin chains serve as general sites of interaction where the sequence variations in the different AB and BC loops provide an array of interaction sites with different specificities and interaction strengths. This could be a mechanism for RACK1 to recruit the ribosome to specific sites in the cytoskeleton and thereby regulate the translation.

Acknowledgements

The authors wish to thank Lise Fismen for her devoted technical assistance and Dr. June H. Myklebust for critical reading of the manuscript. LMM was supported by grants from the Norwegian Cancer Society, project 88066046 and 60365004 and the research council of Norway. AJR was supported in parts by grants from the University of Bergen, project 710028.

REFERENCES

Arimoto K, Fukuda H, Imajoh-Ohmi S, Saito H, Takekawa M. 2008 Formation of stress granules inhibits apoptosis by suppressing stress-responsive MAPK pathways. *Nat. Cell Biol.* **10**: 1324–1332.

Battaini F, Pascale A. 2005. Protein Kinase C Signal Transduction Regulation in Physiological and Pathological Aging. *Ann. N. Y. Acad. Sci.* **1057**: 177–192.

Battaini F, Pascale A, Paoletti R, Govoni S, Battaini F. 1997. The role of anchoring protein rack1 in pkc activation in the ageing rat brain. *Trends Neurosci.* **20**: 410–415.

Begg GE, Harper SL, Morris MB, Speicher DW. 2000. Initiation of Spectrin Dimerization Involves Complementary Electrostatic

Interactions between Paired Triple-helical Bundles. *J. Biol. Chem.* **275**: 3279–3287.
Bennett V, Gilligan DM. 1993. The Spectrin-Based Membrane Skeleton and Micron-Scale Organization of the Plasma Membrane. *Annu. Rev. Cell Biol.* **9**: 27–66.
Ben-Shem A, Jenner L, Yusupova G, Yusupov M. 2010. Crystal Structure of the Eukaryotic Ribosome. *Science* **330**: 1203–1209.
Bjørndal B, Myklebust LM, Rosendal KR, Myromslien FD, Lorens JB, Nolan G, Bruland O, Lillehaug JR. 2007. RACK1 regulates Ki-Ras-mediated signaling and morphological transformation of NIH 3 T3 cells. *Int. J. Cancer* **120**: 961–969.
Bjørndal B, Trave G, Hageberg I, Lillehaug JR, Raae AJ. 2003. Expression and purification of receptor for activated C-kinase 1 (RACK1). *Protein Expr. Purif.* **31**: 47–55.
Bolger G, McCahill A, Yarwood S, Steele M, Warwicker J, Houslay M. 2002. Delineation of RAID1, the RACK1 interaction domain located within the unique N-terminal region of the cAMP-specific phosphodiesterase, PDE4D5. *BMC Biochem.* **3**: 24.
Brenner A, Kieffer B, Travé G, Frøystein N, Raae A. 2012. Thermal stability of chicken brain α-spectrin repeat 17: a spectroscopic study. *J. Biomol. NMR* **53**: 71–83.
Chandramouli P, Topf M, Ménétret J-F, Eswar N, Cannone JJ, Gutell Robin R, Sali A, Akey CW. 2008. Structure of the Mammalian 80S Ribosome at 8.7 Å Resolution. *Structure* **16**: 535–548.
Coyle SM, Gilbert WV, Doudna JA. 2009. Direct Link between RACK1 Function and Localization at the Ribosome In Vivo. *Mol. Cell Biol.* **29**: 1626–1634.
Creighton TE. 1997. Structures and molecular properties, Second edition. W H Freeman and company: New York, page 339.
Diakowski W, Ozimek Ł, Bielska E, Bem S, Langner M, Sikorski AF. 2006. Cholesterol affects spectrin–phospholipid interactions in a manner different from changes resulting from alterations in membrane fluidity due to fatty acyl chain composition. *Biochim. Biophys. Acta (BBA) - Biomembr.* **1758**: 4–12.
Djinovic-Carugo K, Gautel M, Ylänne J, Young P. 2002. The spectrin repeat: a structural platform for cytoskeletal protein assemblies. *FEBS Lett.* **513**: 119–123.
Elgsaeter A, Stokke BT, Mikkelsen A, Branton D. 1986. The molecular basis of erythrocyte shape. *Science* **234**: 1217–1222.
Feng C, Li Y-F, Yau Y-H, Lee H-S, Tang X-Y, Xue Z-H, Zhou Y-C, Lim W-M, Cornvik TC, Ruedl C, Shochat SG, Tan S-M. 2012. Kindlin-3 Mediates Integrin αLβ2 Outside-in Signaling, and It Interacts with Scaffold Protein Receptor for Activated-C Kinase 1 (RACK1). *J. Biol. Chem.* **287**: 10714–10726.
Gaudet R, Bohm A, Sigler PB. 1996. Crystal Structure at 2.4 Å Resolution of the Complex of Transducin βγ and Its Regulator, Phosducin. *Cell* **87**: 577–588.
Gerbasi VR, Weaver CM, Hill S, Friedman DB, Link AJ. 2004. Yeast Asc1p and Mammalian RACK1 Are Functionally Orthologous Core 40S Ribosomal Proteins That Repress Gene Expression. *Mol. Cell Biol.* **24**: 8276–8287.
Grum VL, Li D, MacDonald RI, Mondragón A. 1999. Structures of Two Repeats of Spectrin Suggest Models of Flexibility. *Cell* **98**: 523–535.
Guo J, Wang S, Valerius O, Hall H, Zeng Q, Li J-F, Weston DJ, Ellis BE, Chen J-G. 2011. Involvement of Arabidopsis RACK1 in Protein Translation and Its Regulation by Abscisic Acid. *Plant Physiol.* **155**: 370–383.
Hartwig JH. 1994. Actin-binding proteins 1: spectrin superfamily. *Protein Profile* **1**: 706–778.
He D-Y, Neasta J, Ron D. 2010. Epigenetic Regulation of BDNF Expression via the Scaffolding Protein RACK1. *J. Biol. Chem.* **285**: 19043–19050.
GE Healthcare. Transition state thermodynamic analysis using Biacore T100. **Application Note 80 for Biacore systems**, (https://www.biacore.com/lifesciences/technology/application_notes).
Kolondra A, Lenoir M, Wolny M, Czogalla A, Overduin M, Sikorski AF, Grzybek M. 2010. The role of hydrophobic interactions in ankyrin–spectrin complex formation. *Biochim. Biophys. Acta (BBA) - Biomembr.* **1798**: 2084–2089.
Kundu N, Dozier U, Deslandes L, Somssich IE, Ullah H. 2013. Arabidopsis scaffold protein RACK1A interacts with diverse environmental stress and photosynthesis related proteins. *Plant Signal. Behav.* **8**: e24012.
La-Borde PJ, Stabach PR, Simonović I, Morrow JS, Simonović M. 2010. Ankyrin recognizes both surface character and shape of the 14–15 di-repeat of β-spectrin. *Biochem. Biophys. Res. Commun.* **392**: 490–494.
Lenne PF, Raae AJ, Altmann SM, Saraste M, Hörber JKH. 2000. States and transitions during forced unfolding of a single spectrin repeat. *FEBS Lett.* **476**: 124–128.
Mamidipudi V, Cartwright CA. 2009. A novel pro-apoptotic function of RACK1: suppression of Src activity in the intrinsic and Akt pathways. *Oncogene* **28**: 4421–4433.
McCahill A, Warwicker J, Bolger GB, Houslay MD, Yarwood SJ. 2002. The RACK1 Scaffold Protein: A Dynamic Cog in Cell Response Mechanisms. *Mol. Pharmacol.* **62**: 1261–1273.
Navratilova I, Papalia GA, Rich RL, Bedinger D, Brophy S, Condon B, Deng T, Emerick AW, Guan H-W, Hayden T, Heutmekers T, Hoorelbeke B, McCroskey MC, Murphy MM, Nakagawa T, Parmeggiani F, Qin X, Rebe S, Tomasevic N, Tsang T, Waddell MB, Zhang FF, Leavitt S, Myszka DG. 2007. Thermodynamic benchmark study using Biacore technology. *Anal. Biochem.* **364**: 67–77.
Onishi I, Lin PJC, Diering GH, Williams WP, Numata M. 2007. RACK1 associates with NHE5 in focal adhesions and positively regulates the transporter activity. *Cell. Signal.* **19**: 194–203.
Pascual J, Pfuhl M, Rivas G, Pastore A, Saraste M. 1996. The spectrin repeat folds into a three-helix bundle in solution. *FEBS Lett.* **383**: 201–207.
Pierce BG, Wiehe K, Hwang H, Kim B-H, Vreven T, Weng Z. 2014. ZDOCK server: interactive docking prediction of protein–protein complexes and symmetric multimers. *Bioinformatics* **30**: 1771–1773.
Raae AJ, Bañuelos S, Ylänne J, Olausson T, Goldie KN, Wendt T, Hoenger A, Saraste M. 2003. Actin binding of a minispectrin. *Biochim. Biophys. Acta (BBA) - Protein Proteomics* **1646**: 67–76.
Rabl J, Leibundgut M, Ataide SF, Haag A, Ban N. 2011. Crystal Structure of the Eukaryotic 40S Ribosomal Subunit in Complex with Initiation Factor 1. *Science* **331**: 730–736.
Rich RL, Myszka DG. 2010. Grading the commercial optical biosensor literature—Class of 2008: 'The Mighty Binders'. *J. Mol. Recognit.* **23**: 1–64.
Rodriguez MM, Ron D, Touhara K, Chen C-H, Mochly-Rosen D. 1999. RACK1, a Protein Kinase C Anchoring Protein, Coordinates the Binding of Activated Protein Kinase C and Select Pleckstrin Homology Domains in Vitro†. *Biochemistry* **38**: 13787–13794.
Ruiz Carrillo D, Chandrasekaran R, Nilsson M, Cornvik T, Liew CW, Tan SM, Lescar J. 2012. Structure of human Rack1 protein at a resolution of 2.45 A. *Acta Crystallogr. Sect. F* **68**: 867–872.
Schneidman-Duhovny D, Inbar Y, Nussinov R, Wolfson HJ. 2005. PatchDock and SymmDock: servers for rigid and symmetric docking. *Nucleic Acids Res.* **33**: W363–W367.
Sengupta J, Nilsson J, Gursky R, Spahn CMT, Nissen P, Frank J. 2004. Identification of the versatile scaffold protein RACK1 on the eukaryotic ribosome by cryo-EM. *Nat. Struct. Mol. Biol.* **11**: 957–962.
Sharma G, Pallesen J, Das S, Grassucci R, Langlois R, Hampton CM, Kelly DF, des Georges A, Frank J. 2013. Affinity grid-based cryo-EM of PKC binding to RACK1 on the ribosome. *J. Struct. Biol.* **181**: 190–194.
Shor B, Calaycay J, Rushbrook J, McLeod M. 2003. Cpc2/RACK1 Is a Ribosome-associated Protein That Promotes Efficient Translation in Schizosaccharomyces pombe. *J. Biol. Chem.* **278**: 49119–49128.
Shuman CF, Hämäläinen MD, Danielson UH. 2004. Kinetic and thermodynamic characterization of HIV-1 protease inhibitors. *J. Mol. Recognit.* **17**: 106–119.
Sikorski AF, Hanus-Lorenz B, Jezierski A, Dluzewski AR. 2000. Interaction of membrane skeletal proteins with membrane lipid domain. *Acta Biochim. Pol.* **47**: 565–578.
Sklan EH, Podoly E, Soreq H. 2006. RACK1 has the nerve to act: Structure meets function in the nervous system. *Prog. Neurobiol.* **78**: 117–134.
Smith KJ, Baillie GS, Hyde EI, Li X, Houslay TM, McCahill A, Dunlop AJ, Bolger GB, Klussmann E, Adams DR, Houslay MD. 2007. 1H NMR structural and functional characterisation of a cAMP-specific phosphodiesterase-4D5 (PDE4D5) N-terminal region peptide that disrupts PDE4D5 interaction with the signalling scaffold proteins, βarrestin and RACK1. *Cell. Signal.* **19**: 2612–2624.
Solbak SM, Wray V, Horvli O, Raae AJ, Flydal MI, Henklein P, Henklein P, Nimtz M, Schubert U, Fossen T. 2011. The host-pathogen interaction of human cyclophilin A and HIV-1 Vpr requires specific N-terminal and novel C-terminal domains. *BMC Struct. Biol.* **11**: 49.
Sondek J, Bohm A, Lambright DG, Hamm HE, Sigler PB. 1996. Crystal structure of a GA protein [beta][gamma]dimer at 2.1 A resolution. *Nature* **379**: 369–374.
Speicher DW, Weglarz L, DeSilva TM. 1992. Properties of human red cell spectrin heterodimer (side-to-side) assembly and identification of an essential nucleation site. *J. Biol. Chem.* **267**: 14775–14782.
Steele MR, McCahill A, Thompson DS, MacKenzie C, Isaacs NW, Houslay MD, Bolger GB. 2001. Identification of a surface on the β-propeller protein RACK1 that interacts with the cAMP-specific phosphodiesterase PDE4D5. *Cell. Signal.* **13**: 507–513.

Subauste MC, Ventura-Holman T, Du L, Subauste JS, Chan S-L, Yu VC, Maher JF. 2009. RACK1 down-regulates levels of the pro-apoptotic protein Fem1b in apoptosis-resistant colon cancer cells. *Cancer Biol. Ther.* **8**: 2295–2303.

Svitel J, Boukari H, Van Ryk D, Willson RC, Schuck P. 2007. Probing the Functional Heterogeneity of Surface Binding Sites by Analysis of Experimental Binding Traces and the Effect of Mass Transport Limitation. *Biophys. J.* **92**: 1742–1758.

Tovchigrechko A, Vakser IA. 2006. GRAMM-X public web server for protein–protein docking. *Nucleic Acids Res.* **34**: W310–W314.

Ullah H, Scappini EL, Moon AF, Williams LV, Armstrong DL, Pedersen LC. 2008. Structure of a signal transduction regulator, RACK1, from Arabidopsis thaliana. *Protein Sci.* **17**: 1771–1780.

Viel A, Branton D. 1996. Spectrin: on path from structure to function. *Curr. Opin. Cell Biol.* **8**: 49–55.

Wang W, Huang Y, Zhou Z, Tang R, Zhao W, Zeng L, Xu M, Cheng C, Gu S, Ying K, Xie Y, Mao Y. 2002. Identification and characterization of AGTRAP, a human homolog of murine Angiotensin II Receptor-Associated Protein (Agtrap). *Int. J. Biochem. Cell Biol.* **34**: 93–102.

SUPPORTING INFORMATION

Additional supporting information may be found in the online version of this article at the publisher's web site.